ELSEVIER

Radiotherapy and Oncology 67 (2003) 53–61

RADIOTHERAPY & ONCOLOGY
JOURNAL OF THE EUROPEAN SOCIETY FOR THERAPEUTIC RADIOLOGY AND ONCOLOGY

www.elsevier.com/locate/radonline

In vivo colocalization of 2-nitroimidazole EF5 fluorescence intensity and electron paramagnetic resonance oximetry in mouse tumors

Pierre Mahy[a], Marc De Bast[a], Bernard Gallez[b], John Gueulette[a], Cameron J. Koch[c], Pierre Scalliet[a], Vincent Grégoire[a,*]

[a]*Radiation Oncology Department and Radiobiology Unit, Université catholique de Louvain, St-Luc University Hospital, 10 Avenue Hippocrate, B-1200 Brussels, Belgium*

[b]*Pharmaceutical Sciences Department and Laboratory of Biomedical Magnetic Resonance, Université catholique de Louvain, St-Luc University Hospital, B-1200 Brussels, Belgium*

[c]*Radiation Oncology Department, School of Medicine, University of Pennsylvania, Philadelphia, PA 19104, USA*

Received 5 August 2002; received in revised form 27 December 2002; accepted 24 January 2003

Abstract

Background and purpose: The primary objective of this study was to establish in vivo the relationship between 2-2-nitro-1H-imidazol-1yl-N-(2,2,3,3,3-pentafluoropropyl)-acetamide (EF5) adduct formation and intratumoral oxygen concentrations measured by electron paramagnetic resonance (EPR) in a tumor model mimicking a clinical situation. The secondary objective was an attempt to calibrate in situ the immunofluorescence (IF) signal with EPR oximetry.

Materials and methods: IM syngeneic fibrosarcoma (NFSA) bearing C3H mice were used. Three days after injection of a paramagnetic charcoal into the tumor, the mice were anesthetized, injected with the hypoxic marker EF5, and monitored every 20 min for 3 h with a low-frequency EPR spectrometer. Animals were allowed to breath either under 21 or 100% O_2. Tumors were then harvested, frozen, cut into sections including the charcoal and processed for EF5 adducts detection using monoclonal antibodies. Slices were viewed with a fluorescence microscope and 190 × 140 μm areas surrounding the charcoal were digitized and analyzed with the NIH-Image and Adobe Photoshop™ software. The fluorescence intensity (FI) was measured in the whole pictures and in strips of 10 μm around the charcoal.

Results: EF5 binding increased with decreasing pO_2, most substantially at pO_2 below 5 mm Hg. Baseline (ambient air) pO_2 reached 3.2 ± 2.1 mm Hg in NFSA tumors. It increased to 9.8 ± 3.2 mm Hg under 100% O_2. A statistically significant correlation was observed on an individual tumor basis between the FI in the first 10 μm strip around the charcoal and the pO_2 determined by EPR oximetry (Wilcoxon signed rank test: $P < 0.001$).

Conclusions: The present study confirms the intrinsic relationship between EF5 adduct binding and intratumoral pO_2 in an in vivo environment under biologically-relevant pO_2 values of less than 10 mm Hg.

© 2003 Elsevier Science Ireland Ltd. All rights reserved.

Keywords: Tumor hypoxia; Nitroimidazole markers; 2-2-nitro-1H-imidazol-1yl-N-(2,2,3,3,3-pentafluoropropyl)-acetamide; Immunofluorescence; Electron paramagnetic resonance

1. Introduction

Hypoxia has been known for a long time to be an important physiological parameter in tumor growth and response to therapy. Experimental and clinical evidences suggest that the hypoxic fraction in solid tumors may: (1) influence tumor growth; (2) increase the malignant phenotype; (3) enhance the metastatic potential due to gene amplification; and (4) reduce the sensitivity to various treatment modalities (e.g. sparsely ionizing radiation and some chemotherapeutic agents) [18,34,44,47,48,50]. Therefore assessment of tumor hypoxia may have profound therapeutic implications in oncology. Techniques able to determine the hypoxic fraction of human tumors in clinical conditions are thus needed.

Among various techniques able to detect hypoxia (see review in Ref. [45]), polarographic measurement (e.g. Eppendorf probe) is the only method for which a correlation to treatment outcome has been extensively demonstrated in different human tumor types, e.g. cervix, head and neck

* Corresponding author.

0167-8140/03/$ - see front matter © 2003 Elsevier Science Ireland Ltd. All rights reserved.
doi:10.1016/S0167-8140(03)00028-8

lymph nodes, sarcoma [3,13,17]. Nevertheless, until now, this technique has not spread to clinical routine due to its relatively low sensitivity at low oxygen concentrations and some logistic constraints. The use of the so-called 'hypoxic cell chemical markers' represents an attractive alternative to polarographic measurements (see review in Ref. [41]). These markers are nitroheterocyclic compounds, which exhibit a particular metabolism under hypoxic cellular conditions. Addition of the first electron occurs irrespective of the oxygen concentration by various reductase systems, e.g. cytochrome P450 reductase, quinone oxydoreductase, xanthine oxydase. Under hypoxic conditions, further reduction steps on the nitro group occurs and the so-derived moieties covalently bound to intracellular macromolecules, mainly to thiol-containing proteins [40]. These reduced moieties trapped into hypoxic cells, can be detected by immunohistochemistry [26] or immunofluorescence (IF) [6] on tissue sections or by flow cytometry on cell suspension [19,27], using for all these techniques specific antibodies. Tagged with an appropriate radioactive isotope, these reduced moieties can be detected by nuclear medicine techniques [10,43]. Binding assays with the 2-nitroimidazole compounds have a maximum sensitivity at low pO_2 concentrations (<10 mm Hg) and are not influenced by tissue necrosis where drugs are not metabolized.

Pimonidazole is one nitroimidazole derivative, which has been extensively studied in pre-clinical models and for which in situ binding in human cervix and head and neck carcinoma has been already reported [2,26]. A recent report strongly suggested that pimonidazole binding could predict for treatment outcome of head and neck squamous cell carcinoma [23].

2-2-nitro-1H-imidazol-1yl-N-(2,2,3,3,3-pentafluoropropyl)-acetamide (EF5) is another nitroimidazole derivative, which allows specific and sensitive detection of tissue hypoxia by flow cytometry and by IF both in in vitro and in vivo settings [6–8,27,31]. EF5 binding in human squamous cell carcinoma of the cervix and the head and neck, and in sarcoma has been recently reported [9,11,28]. In vitro, maximum sensitivity for EF5 binding was observed for oxygen concentrations below 10 mm Hg [27]. EF5 is remarkably stable in vivo. It is substantially lipophilic, and hence has an even biodistribution in animal models [29]. The presence of five fluorine atoms on the side chain provides an excellent hapten for the development of specific monoclonal antibody against EF5 adducts [31]. Furthermore it permits the labeling of one of these fluorine atoms by a [^{18}F] positron emitter isotope. This tracer would retain all the properties of the unlabeled parent compound, irrespective of the position of the labeled fluorine. Successful synthesis of the mono-fluorine ([^{18}F]-EF1), the tri-fluorine ([^{18}F]-EF3) and the penta-fluorine ([^{18}F]-EF5) derivatives of etanidazole have been reported [5,10,22,24]. Despite belonging to the same family, these derivatives present different lipophilicity, which is likely to impact on the biodistribution. Although binding assays with nitroimidazole compounds offer an elegant way to assess tissue hypoxia, they however only permit a relative quantitation of hypoxia, thus limiting interpretation and comparison of multicentric data.

Electron paramagnetic resonance (EPR) oximetry is another method for measuring tissue hypoxia in vitro and in vivo [32]. EPR oximetry is based on the broadening of the resonance spectrum of a paramagnetic material by oxygen. Recent progress made both in the instrumentation and in the paramagnetic materials allows absolute measurements of pO_2 in tissues with an accuracy and sensitivity comparable or greater to that available by any other methods [46]. It has been demonstrated that EPR oximetry is a convenient method for measuring pO_2 in murine tumors in the range of 0–30 mm Hg [1] as well as for understanding the timing of tumor reoxygenation after irradiation [14,38]. A new paramagnetic material, which is able to detect very subtle changes of pO_2 in tissue was recently characterized in our institution [21] and used for monitoring pharmacologically-induced modifications of tumor pO_2 [12]. This material is sensitive to variations of pO_2 of less than 1 mm Hg and possesses a high spin density providing a high signal to noise ratio in the EPR measurements carried out in vivo. EPR oximetry however requires the intravenous or intratumoral injection of a paramagnetic substance into the tumor, and with the instrumentation available today (spectrometers working at a frequency of 1 GHz), resonance spectrum can only be acquired for material implanted not deeper than 10 mm.

From a clinical point of view, the only methods for tumor hypoxia determination that could be used on a routine basis and thus impact on patient care, are those which are highly specific to hypoxia, minimally or non-invasive, sensitive in the range of pO_2 below 10 mm Hg and, ideally, available for all tumor sites. As yet, binding assays with nitroimidazole compounds appear to offer the best prospect to fulfill these requirements. However, as already mentioned, binding assays only permit a relative quantitation of hypoxia. Yet multicentric studies will be required to validate the use of hypoxia as a prognostic factor upon which therapeutic interventions against hypoxia will be elaborated.

In this framework, we investigated the relation between hypoxia binding assay with EF5 and absolute oximetry with EPR using colocalization of the two methods in a mouse tumor model. The primary objective was to establish in vivo the relationship between EF5 adduct formation and intratumoral oxygen concentrations in a tumor model mimicking a clinical situation. The secondary objective was an attempt to calibrate in situ the IF signal with EPR oximetry.

2. Materials and methods

2.1. Drug and antibody

The pentafluorinated nitroimidazole derivative EF5

designed by C.J. Koch was used as an hypoxic marker for the binding assay [6,31]. The EF5 adduct specific monoclonal antibody ELK3-51 conjugated to the fluorescent dye Cy-3 was synthesized by E. Lord [31]. Both EF5 and antibody were kindly provided by C.J. Koch. A 10 mM EF5 solution in 0.9% saline was prepared before each set of experiments.

2.2. Animal and tumor model

Eight–12 week old male C3H/HeOuJlco mice purchased from IFFA CREDO Belgium were housed four per cage and were given food and water ad libitum for the duration of the experiments. Animals were maintained in a facility approved by the Belgian Ministry of Agriculture in accordance with current regulations and standards. Experimental design was approved by the ethics committee on animal experimentations of the School of Medicine of the Université catholique de Louvain.

The NFSA fibrosarcoma syngeneic to C3Hf/Kam mice was kindly provided by L. Milas from the University of Texas, M.D. Anderson Cancer Center, Houston, USA. Maintenance and expansion of the tumor line in vivo have been previously described [35]. Briefly, tumor cells from the third isotransplant generation in our laboratory were injected into the mouse flank to generate tumor sources. Single cell suspensions of excised tumors were prepared by trypsin and DNAse digestion of non-necrotic tissue. The cell viability evaluated by Trypan blue dye exclusion under phase-contrast microscopy was around 70%. Tumors were generated by injection in the gastronecmius muscle of 10^6 cells in 10–20 μl of McCoy medium. Tumor growth was determined by daily measurements of three orthogonal diameters with a caliper.

2.3. Electron paramagnetic resonance oximetry

The intratumor oxygen partial pressure was monitored using an EPR spectrometer (Magnettech, Berlin, Germany) with a low frequency microwave bridge operating at 1.2 GHz and an extended loop resonator (1 cm depth sensitivity) designed and built by Dr. T. Walczak (Darmouth Medical School, Hanover, USA) [37]. A paramagnetic charcoal (charcoal wood powder, CX0670-1, EM Science, Gibbstown, USA) dispersed in phosphate-buffered saline (PBS) was used as the oxygen-sensitive probe. The diameter of the charcoal particles was less than 25 μm with mean values of 3–5 μm. Calibration curve was made as previously described by measuring in vitro the EPR linewidth as a function of pO_2 [21]. When tumors reached a mean diameter ± SD of 8.4 ± 0.6 mm, 20 μl of a 100 mg/ml suspension of the paramagnetic substance was injected into the tumor with a 25 gauge needle. Three to four days later when tumors have reached a mean ± SD diameter of 10.6 ± 0.8 mm, the mice were anesthetized with 140 mg/kg ketamine (Ketalar®, Parke-Davis, Warner-Lambert S.A., Belgium) and 1.3 mg/kg xylazine (Rompun®, Bayer AG, Germany) and placed in the magnetic field with the loop resonator wrapping the tumor or the lower limb. Anesthesia was repeated using half dose between 60 min and 90 min after the start of the experiment. Intratumor oxygen partial pressure was monitored every 20 min for 3 h. For each measurement, the typical acquisition time varied between 1 and 5 min to generate spectra with adequate signal-to-noise ratio. The modulation amplitude was lower than one third of the EPR linewidth. For each tumor, the mean pO_2 was determined by averaging the various measurements. To broaden the difference in intratumor oxygen partial pressure between animals, mice were allowed to breath under 21% (ambient conditions) or 100% O_2 concentration during the 3 h of monitoring. For that purpose, oxygen flowed at a constant rate (2 l/min) through a 50 ml syringe covering the head of the animal. Body temperature was not monitored during experiments.

2.4. EF5 binding assay

EF5 was administered to anesthetized mice just before starting the EPR oximetry and oxygen flow if required. EF5 was injected in the tail vein at a dose resulting in a whole body concentration of 100 μM. Three hours after injection, animals were sacrificed by cranio-cervical dislocation. Tumors were harvested, coated with Tissue-Tek® OCT Compound (Sakura Finetek Inc., Torrance, USA), plunged into 100% ethanol and frozen in liquid nitrogen for 30 s. Tumors were then dry-stored at −80 °C until processing. Frozen tumors were cut in the region where the charcoal was implanted in 8 μm thick sections using a HM 500 M cryostat (Microm Laborgeräte GmbH, Walldorf, Germany). An average of 5–8 sections were obtained per tumor. Sections were then processed for IF staining as previously described [6]. Briefly, sections were fixed for 1 h with 4% paraformaldehyde in PBS, and rinsed twice in PBS. Sections were blocked overnight with 5% mouse serum in PBS with 0.3% Polyoxyethylenesorbitanmonolaurate (Tween 20) and rinsed first in PBS then in PBS with 0.3% Tween 20. Sections were then stained for 6 h with 75 μg/ml Cy-3 conjugated ELK3-51 monoclonal antibody in PBS with 0.3% Tween 20 and 1.5% bovine albumin. After rinsing twice in PBS with 0.3% Tween 20 and once in PBS, sections were stored in PBS with 1% paraformaldehyde until image acquisition. All steps were performed at 4 °C. After image acquisition, sections were counterstained with Haematoxylin and Eosin. For each tumor, one section was incubated with the vehicle only and used as negative control of tissue background fluorescence. Tumor sections from mice having no EF5 were also stained and used as negative controls to assess the non-specific binding of the antibody.

2.5. Image acquisition

Sections were visualized with an epi-fluorescence

microscope (Zeiss, Berlin, Germany) equipped with a stabilized power supply, a 60 W mercury arc bulb, a fluorescein isothiocyanate (FITC)-Rhodamine excitation filter, a dichroic mirror and a 590 nm pass barrier emission filter. A DXC-950P CCD camera (Sony Corporation, Tokyo, Japan) with a sensitivity of f 8.5 at 2000 lux, a signal-to-noise ratio of 58 db, and a minimum illumination of 6.5 lux was mounted on the microscope. The CCD camera was connected to a Power Macintosh 4400 with a frame grabber (CG-7, Scion Corporation, Frederick, USA), and the images were acquired using the public domain NIH Image software (developed at the U.S. National Institute of Health and available on the Internet at http://rsb.info.nih.gov:nih-image). Pictures were saved as TIFF files. Images were acquired through a Zeiss Neofluar 40 × objective (N = 0.75), an additional 1.25 × lens and a camera adapter. Resulting images covered an area of 190 × 140 μm. An average ± SD of 52 ± 12 haphazardly chosen microscopic fields were digitized in the tumor region contiguous to the charcoal edge. To determine the relative area occupied by the charcoal and the tumor in each field, incandescent backlighting was performed after each fluorescence acquisition and the resulting images were digitized. During photography, to avoid tissue desiccation and provide an uniform optical path, a space around the sections was delineated with mylar tape, filled with 1% paraformaldehyde in PBS and covered with a coverslip. To correct for variations in the intensity of the mercury bulb lighting, images of a Cy-3 solution filling a Malassez hemocytometer were acquired before each acquisition of tumor sections [8]. The gain of the CCD camera was adjusted to set the mean fluorescence intensity (FI) of the Cy-3 solution at 235 on a 0–255 -8bits- scale.

2.6. Data analysis

Digitized images were analyzed with Adobe Photoshop 3™ software. Considering the emission spectra of Cy-3 in the red spectrum, to increase the signal-to-noise ratio, only the red component of the computerized Red–Green–Blue TIFF file of each picture was analyzed.

Respective tumor and charcoal areas were delineated in the fluorescence pictures using the colocalized backlighted pictures. The FI was measured in whole tumor area and in strips ranging from 0 to 10, 10 to 20 and 20 to 30 μm around the charcoal. These strips were automatically delineated by expanding the surface occupied by the charcoal by 10, 20 or 30 μm. We have shown that murine tumors had almost no autofluorescence (tumors with EF5 and without antibody), and consequently correction in FI were only made for non-specific antibody binding by subtracting the FI of control samples processed on the same day (tumors without EF5 and with antibody staining).

2.7. Statistical analysis

Statistical difference between two groups of unpaired data (e.g. EPR oximetry in 21% vs. 100% O_2 tumors) was assessed using one-tailed *t*-test on the mean. As EPR oximetry measurements and IF values were obtained from the same individual tumors, paired tests had to be used to calculate correlation between the two assays. Because of the low number of tumors (<20), the Student paired *t*-test could not be used and the Wilcoxon signed-rank test was thus chosen. It allows analysis of paired continuous variables in small samples ($n < 20$) when the distribution of the differences cannot be assumed gaussian (Kurtosis or $\propto^4 \neq 0$) but is symmetrical (Skewness or $\propto^3 \approx 0$). This test is however less powerful than the Student paired *t*-test. Relation between EPR oximetry measurements and IF values was also classically estimated by the Bravais–Pearson coefficient of correlation.

3. Results

3.1. Effect of charcoal on tumor physiology

After injection, no statistical difference ($P > 0.2$) was observed between the tumor volume doubling time of charcoal-injected tumors (mean ± SEM of 8.3 ± 0.4 days, $n = 25$) and of control tumors (mean ± SEM of 9.2 ± 0.5 days, $n = 24$), which confirms previously reported study [38]. No necrosis around charcoal was found after careful pathological examination of all Hematoxylin–Eosin stained sections.

3.2. Electron paramagnetic resonance oximetry

In a preliminary experiment, it has been shown that after induction of the anesthesia and modification of the breathing condition, the intratumoral pO_2 raised almost immediately and leveled off from 20–40 min on (Fig. 1). In the muscles, stabilization of the pO_2 was reached within 5 min (data not shown). Therefore, it was decided to record EPR oximetry every 20 min during the whole period of EF5 metabolism starting at 20 min after injection up to 160 min to allow sacrifice of the animals exactly at 3 h.

The charcoal was injected into 25 tumor bearing mice which were all processed for EPR oximetry. No EPR signal could be detected in four mice: post mortem dissection of the tumors showed a lack of charcoal injection in three mice. In the remaining mouse, the loop resonator could not be correctly placed around the tumor, which was implanted high in the thigh. In the 21 mice for whom adequate EPR spectra were obtained, five tumors were discarded after the pathological examination had shown that the charcoal was not entirely implanted into the tumors. In these mice, the EPR spectra could have been influenced by the pO_2 from the muscle surrounding the tumor.

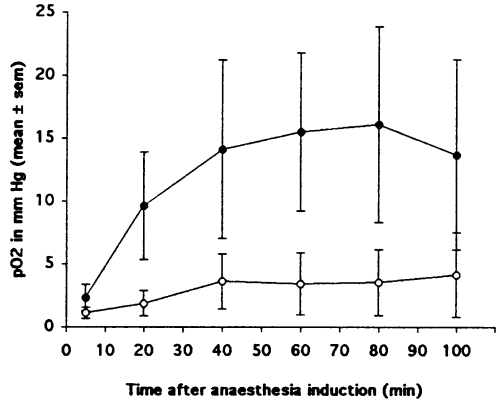

Fig. 1. In vivo EPR oximetry in NFSA tumor bearing mice breathing 21% O_2 (○, $n = 5$) or 100% O_2 (●, $n = 7$). Anesthesia (IP injection of Ketamine–Xylazine) and breathing of 100% O_2 started at time zero.

Large variability in pO_2 was detected among the 16 NFSA tumors from mice breathing 21% or 100% O_2 concentrations (Fig. 2). Average pO_2 values during the 3 h of experiment spread between a maximum of 38.6 mm Hg and a minimum and 0.1 mm Hg. On average, under ambient air conditions ($n = 5$), NFSA tumors were highly hypoxic with a mean ± SEM of 3.2 ± 2.1 mm Hg. Under 100% O_2 concentrations ($n = 11$), the pO_2 was typically higher with a mean ± SEM of 9.8 ± 3.2 mm Hg. However, not every mice responded to pure oxygen breathing. Three tumors remained hypoxic despite hyperoxygenation, reaching values of 0.1, 1.1, and 1.4 mm Hg. Despite high tumor

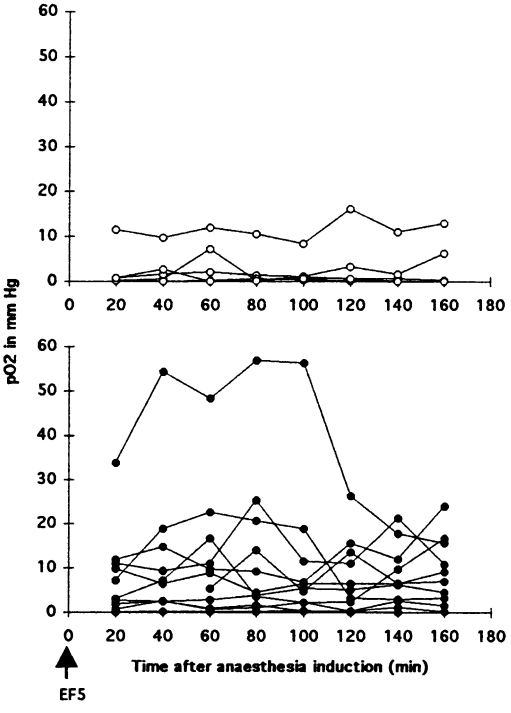

Fig. 2. In vivo EPR oximetry in NFSA tumor bearing mice under 21% O_2 (top panel) or under 100% O_2 (bottom panel); anesthesia (IP injection of Ketamine–Xylazine), EF5 injection and breathing of 100% O_2 started at time 0.

heterogeneity, the difference between the 100% O_2 and 21% O_2 groups reached a borderline level of significance (one-tailed t-test, $P = 0.054$). Nevertheless, during the 3 h EPR measurements, the intra-tumor coefficient of variation (average of 75%) was lower than the inter-tumor coefficient of variation (average of 125%).

3.3. Hypoxia determined by EF5 immunofluorescence

EF5 binding was determined in the 16 tumors for which adequate pO_2 determination was obtained with EPR. Large variations in FI were obtained in NFSA tumor bearing mice breathing 21% or 100% O_2. In animals breathing ambient conditions, average FI ± SEM in the whole tumor area reached 23.4 ± 6.2. Corresponding value in animals breathing 100% O_2 reached 12.4 ± 4. Due to large heterogeneity among samples, the difference between the two groups did not reach a level of significance (one-tailed t-test, $P = 0.09$). It is noteworthy to mention that the three tumors remaining hypoxic despite hyperoxygenation showed high EF5 binding. In these tumors, average FI ± SEM reached 16 ± 1.7, 18.7 ± 1.6 and 47.6 ± 9.4 for EPR oximetry of 1.4 ± 0.3, 0.1 ± 0.004 and 1.1 ± 0.3 mm Hg, respectively.

3.4. Influence on the measurement area on the determination of hypoxia with EF5

The objective of this study was to establish the in vivo relationship between EF5 binding and EPR oximetry using colocalization of the two assays. It is assumed that the EPR spectra are mainly influenced by the oxygen concentration at the interface between the charcoal and the tumor. As already described in Section 2, for the EF5 binding assay, the FI was determined from pictures of 190 × 140 μm after subtraction of the charcoal area. As physiological pO_2 variations might occur over such distances, the FI was measured in whole tumor area but also in strips distant from 0 to 10, 10 to 20 and 20 to 30 μm of the charcoal edges, corresponding grossly to first, second and third cells layer wrapped around the charcoal. No systematic difference in the FI between the various strips analyzed could be demonstrated (Table 1).

3.5. Relationship between EF5 immunofluorescence and electron paramagnetic resonance oximetry

For each of the 16 tumors, for which both EPR oximetry and IF were available, the two assays were plotted against each other (Fig. 3). For the EF5 FI, despite the systematic absence of variation throughout the picture as demonstrated in Table 1, only the first 10 μm strip around the charcoal was taken into consideration. A statistically significant correlation was observed on individual tumor basis between EPR oximetry and EF5 adduct FI (Wilcoxon signed rank test: $P = 0.001$). Data points were better fitted through a logarithmic curve than a linear trendline ($r^2 = 0.54$,

Table 1
EPR oximetry and fluorescence intensity (corrected for non-specific binding of the antibody) in tumor layers of 10 μm width around charcoal[a]

	Breathing conditions	mean FI ± SEM (EF5)			mean pO_2 ± SEM (EPR)
		0–10 μm	10–20 μm	20–30 μm	
Tumor 1	Air	23.81 ± 1.77	26.89 ± 2.18	26.58 ± 2.19	0.2 ± 0.07
Tumor 2	Air	37.65 ± 3.32	42.19 ± 3.84	42.99 ± 4.00	0.6 ± 0.30
Tumor 3	Air	21.13 ± 3.96	20.45 ± 3.95	23.75 ± 4.51	2.18 ± 0.63
Tumor 4	Air	15.9 ± 3.32	23.84 ± 3.78	31.76 ± 5.57	1.33 ± 0.84
Tumor 5	Air	1.75 ± 0.63	1.65 ± 0.65	2.33 ± 1.02	11.48 ± 0.82
Tumor 6	Oxygen	8.79 ± 3.00	14.74 ± 3.51	16.53 ± 3.54	3.97 ± 0.55
Tumor 7	Oxygen	11.08 ± 1.74	18.05 ± 3.16	20.66 ± 3.96	1.42 ± 0.32
Tumor 8	Oxygen	14.89 ± 1.40	18.14 ± 1.60	18.99 ± 1.70	0.15 ± 0.05
Tumor 9	Oxygen	8.48 ± 0.45	7.99 ± 0.44	6.49 ± 0.53	7.62 ± 2.17
Tumor 10	Oxygen	10 ± 0.81	9.74 ± 0.75	12.26 ± 0.81	13.86 ± 2.09
Tumor 11	Oxygen	2.53 ± 0.99	3.27 ± 1.03	4.51 ± 1.47	12.93 ± 1.87
Tumor 12	Oxygen	9.62 ± 0.47	9.79 ± 0.52	8.15 ± 0.56	12.14 ± 3.12
Tumor 13	Oxygen	3.30 ± 1.29	7.70 ± 2.11	11.55 ± 2.95	8.49 ± 1.70
Tumor 14	Oxygen	0.44 ± 0.21	0.43 ± 0.21	0.37 ± 0.18	7.18 ± 0.64
Tumor 15	Oxygen	0.00 ± 0.00	0.19 ± 0.18	0.65 ± 0.45	38.62 ± 6.17
Tumor 16	Oxygen	29.18 ± 8.95	44.51 ± 9.46	54.17 ± 9.54	1.14 ± 0.35

[a] No systematic difference was observed between the three layers.

$P < 0.01$ and $r^2 = 0.36$, $P < 0.02$, respectively). The data point outside of the linearity range of EPR oximetry (0–30 mm Hg) was not discarded from the plot. EF5 binding mainly occurred in tumors considered as hypoxic with EPR oximetry. For instance, average FI ± SEM) for tumors with pO_2 below 10 mm Hg was significantly higher than for those above 10 mm Hg (15.88 ± 3.39 vs. 4.78 ± 2.1, $P = 0.027$). Using a cutoff value of 5 mm Hg, the difference in FI between the two groups reached an even higher level of significance (20.3 ± 3.43 vs. 4.52 ± 1.48, $P = 0.0004$).

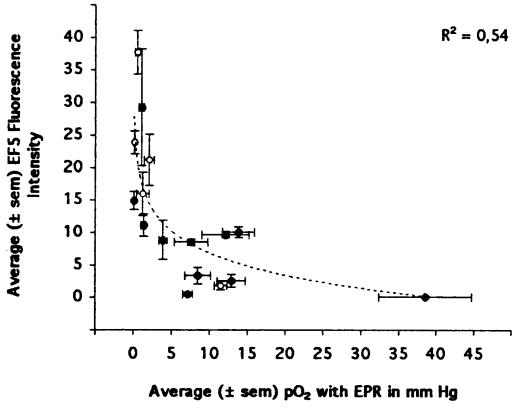

Fig. 3. In vivo correlation between EPR oximetry and EF5 immunofluorescence in individual NFSA tumors (Wilcoxon signed-rank test $P < 0.001$; Bravais–Pearson coefficient of correlation $r^2 = 0.54$, $P < 0.01$). Mice were allowed to breath 21% (○, $n = 5$) or 100% (●, $n = 11$) O_2 during the 3 h EF5 metabolism and EPR oximetry. Each dot is the average ± SEM of EPR measurements performed every 20 min for 3 h, and the average ± SEM FI on a 10 μm strip around the charcoal.

4. Discussion

The primary objective of our study was to establish in vivo the relationship between EF5 adduct binding and intratumoral pO_2. In a mouse fibrosarcoma model, our data demonstrated a statistically significant correlation between EF5 binding and EPR oximetry on an individual tumor basis (Fig. 3).

The relationship between EF5 binding and pO_2 is at the basis for the use of this chemical as hypoxia marker. Comprehensive in vitro studies on tumor cell suspensions and multicell tumor spheroids have already demonstrated an inverse correlation between EF5 adduct binding and oxygen concentration [7,27,49]. Such binding occurred over a wide dynamic range greater than 100, and, in comparison with other nitroimidazole compound (e.g. misonidazole), it has been shown to be highly specific to oxygen concentration [27]. In vivo, a weak correlation has been reported between intratumoral pO_2 measured with Eppendorf electrodes and EF5 binding measured by flow cytometry on single cell suspension [25]. However, as the two methods were not colocalized, such data need cautious interpretation. Furthermore, it is known that Eppendorf measurements have a low sensitivity at low pO_2 values and that the readings are influenced by tumor necrosis [20].

In the present study, EF5 binding was colocalized with EPR oximetry used as a sensitive and specific method to measure oxygen concentration during the 3 h of EF5 metabolism. In the design of our study, it was assumed that EF5 binding was influenced by the average pO_2 value during the 3 h metabolism. This explains why the EPR oximetry was also averaged over 3 h. As observed in Figs. 1 and 2, stability of the EPR readings occurred mainly after 20 min, which is likely the time required for a complete

biodistribution of EF5. Indeed, for EF3, a slightly more hydrophylic derivative of etanidazole, it has been reported that 30 min was required for adduct formation [4]. EF5 binding occurred for pO_2 below 10 mm Hg, increasing mostly for pO_2 below 5 mm Hg, confirming the low K_m value estimated in vitro with EF5 [8,27] but also with other nitroimidazole compound such as misonidazole or NITP [15,19]. In vivo, Raleigh et al. found a better correlation between pimonidazole binding and the percentage of pO_2 values below 2.5, 5 or 10 mm Hg (r^2 of 0.83, 0.82, 0.81) measured with an Eppendorf probe than between pimonidazole binding and the mean or median pO_2 values (r^2 of 0.58, 0.54) [42]. Indirectly, this study, in agreement with our data, demonstrated that nitroimidazole compounds detect in vivo 'hot spots' of hypoxia at pertinent levels of pO_2 below 10 mm Hg. As variation of radiosensitivity occurs at very low pO_2 mainly below 10 mm Hg [16], it is thus not surprising that excellent correlation between EF5 binding and paired cell survival assays could be demonstrated [7,25,30].

One possible limitation of the present study lies in the difference between the measurement area by EPR and by the EF5 binding assay. Whereas EF5 binding can be precisely located at the cellular level, it is still unclear which tumor volume is averaged by the EPR measurement. It is thought that the EPR spectrum depends on the oxygen concentration at the interface between the charcoal implant and the surrounding tumor [46]. In a three-dimensional view, it is thus likely that EPR measures an average pO_2 in the whole 20 μl volume of the charcoal implant which is an agglomerate of several 3–5 μm granules between which oxygen can freely diffuse. That is why in the present experiments, EF5 FI was averaged over a 10μm distance from the charcoal edge, which is likely to correspond to the first cell layer surrounding the charcoal implant. Anyway, under the experimental setting used in the present study, no significant difference in FI was observed between the first, second and third 10μm strip around the charcoal (Table 1). This observation suggests that in our NFSA tumor model, there was no systematic pO_2 gradient around the charcoal implants at least over a 30 μm distance. Local variations of oxygenation have been reported around sites of intratumoral injections with a 26 gauge needle [39]. In our tumor model and experimental conditions, it is likely that even if such variations occurred immediately after injection, the 3-day delay before measurements allowed a return to baseline conditions. Along this line, we have shown that when EPR measurements are performed in the muscle on a day to day basis, stable pO_2 values are reached at the 3rd day after charcoal injection (data not shown). Also, on the contrary to what could happens with the use of infusible paramagnetic substance, EPR measurements after charcoal implant is not biased by the lack of signal in non-perfused areas [33]. So, despite the technical difficulties of a 3-dimensional determination of EF5 binding around all the granules of the charcoal implant, the method used in the present study is probably the most detailed in vivo colocalization attempt to date.

The secondary objective of our study was to potentially calibrate the immunofluorescence signal intensity using the relationship between EF5 binding and EPR oximetry. In the present study, EF5 adducts were measured by the fluorescence intensity. The use of direct fluorescence with a Cy-3 conjugated antibody provides indeed a signal directly proportional to the amount of EF5 adducts, and thus permits a more accurate quantitation of the hypoxic fraction [27]. However, due to scattering in the data, especially for pO_2 values above 5 mm of Hg, it is still uncertain how such relationship could be of practical value. In addition, whether this curve would hold for various tumor types and tissue processing still needs to be further investigated. For the proof of principle, the NFSA tumor model type was chosen in the present study for various reasons. First, NFSA is a relatively firm tumor, which allowed the charcoal implants to remain as clusters at the site of injection. Second, we have shown that the charcoal implants did not modify the tumor growth and did not trigger any inflammatory reaction around the granules, at least on the 3rd day after charcoal injection. Third, NFSA tumors have been reported to have a low necrotic fraction around 0.2% for 8 mm diameter tumor [36]. In principle, neither of these characteristics (except the absence of an inflammatory shell around the charcoal) is required to validate the inherent relationship between EF5 binding and intratumoral pO_2 in vivo, but tumor models lacking these features would certainly be more difficult to process and to analyze, and consequently might introduce heterogeneity in the calibration curve. Whatsoever, the only requirement would be to use a similar methodology throughout all the experimental steps, especially for the EF5 binding assay.

One alternative to calibrate the EF5 FI is to process on the same tumor section a small cluster of fixed cells incubated with EF5 in vitro at a given pO_2, which could be used as external control of absolute pO_2 in absence of EPR oximetry. Such solution might be more adequate for comparison of multi-institutional data.

Acknowledgements

This work was supported by research grants from the 'Fonds de la Recherche Scientifique Médicale' (grants # 3.4571.95, 3.4610.99 and 3.4560.00) of Belgium and by grants from the 'Fonds Joseph Maisin', Brussels, Belgium. The authors thank Mrs Michèle Octave-Prignot for statistical assistance and Prof. Luka Milas and Prof. Hervé Reychler for their advice, their encouragements and the fruitful discussions during the acquisition and the analysis of the data.

References

[1] Bacic G, Liu KJ, O'Hara JA, et al. Oxygen tension in a murine tumor: a combined EPR and MRI study. Magn Reson Med 1993;30:568–72.

[2] Begg AC, Janssen H, Sprong D, et al. Hypoxia and perfusion measurements in human tumors–initial experience with pimonidazole and IUdR. Acta Oncol 2001;40:924–8.

[3] Brizel D, Scully SP, Harrelson JM, et al. Tumor oxygenation predicts for the likelihood of distant metastases in human soft tissue sarcoma. Cancer Res 1996;56:941–3.

[4] Busch TM, Hahn SM, Evans SM, Koch CJ. Depletion of tumor oxygenation during photodynamic therapy: detection by the hypoxia marker EF3 [2-(2-nitroimidazol-1[H]-yl)-N-(3,3,3-trifluoropropyl)acetamide]. Cancer Res 2000;60:2636–42.

[5] Dolbier WR, Li AR, Koch CJ, Shiue CY, Kachur AV. [^{18}F]-EF5, a marker for PET detection of hypoxia: synthesis of a precursor and a new fluorination procedure. Appl Radiat Isot 2001;54:73–80.

[6] Evans SM, Joiner B, Jenkins WT, Laughlin KM, Lord EM, Koch CJ. Identification of hypoxia in cells and tissues of epigastric 9L rat glioma using EF5 [2-(2-nitro-1H-imidazol-1yl)-N-(2,2,3,3,3-pentafluoropropyl)acetamide]. Br J Cancer 1995;72:875–82.

[7] Evans SM, Jenkins WT, Joiner B, Lord EM, Koch CJ. 2-Nitromidazole (EF5) binding predicts radiation resistance in individual 9L s.c. tumors. Cancer Res 1996;56:405–11.

[8] Evans SM, Koch CJ, Laughlin KM, Jenkins WT, van Winkle T, Wilson DF. Tamoxifen induces Hypoxia in MCF-7 xenografts. Cancer Res 1997;57:5155–61.

[9] Evans SM, Hahn S, Pook DR, et al. Detection of hypoxia in human squamous cell carcinoma by EF5 binding. Cancer Res 2000;60: 2018–24.

[10] Evans SM, Kachur AV, Shiue CA, et al. Noninvasive detection of tumor hypoxia using the 2-nitroimidazole [^{18}F]EF1. Nucl Med 2000; 41:327–36.

[11] Evans SM, Hahn SM, Magarelli DP, et al. Hypoxia in human intraperitoneal and extremity sarcomas. Int J Radiat Oncol Biol Phys 2001;49:587–96.

[12] Gallez B, Jordan BF, Baudelet C, Misson PD. Pharmacological modifications of the partial pressure of oxygen in tumors: evaluation using in vivo EPR oximetry. Magn Reson Med 1999;42:627–30.

[13] Gatenby RA, Kessler HB, Rosenblaum JS, et al. Oxygen distribution in squamous cell carcinoma mestastases and its relationship to outcome of radiation therapy. Int J Radiat Oncol Biol Phys 1988;14: 831–8.

[14] Goda F, Bacic G, O'Hara JA, Gallez B, Swartz HM, Dunn JF. The relationship between partial pressure of oxygen and perfusion in two murine tumors after X-Ray irradiation: a combined gadopentetate dimeglumine dynamic magnetic resonance imaging and in vivo electron paramagnetic resonance oximetry study. Cancer Res 1996; 56:3344–9.

[15] Gross MW, Karbach U, Groebe K, Franko AJ, Mueller-Klieser W. Calibration of misonidazole labeling by simultaneous measurements of oxygen tension and labeling density in multicellular spheroids. Int J Cancer 1995;61:567–73.

[16] Hall EJ. The oxygen effect and reoxygenation. In: Hall EJ, editor. Radiobiology for the radiologists. Philadelphia: J. B. Lippincott Company, 1994. p. 133–52.

[17] Hockel M, Schlenger K, Aral B, Mitze M, Schaffer U, Vaupel P. Association between tumor hypoxia and malignant progression in advanced cancer of the uterine cervix. Cancer Res 1996;56:4509–15.

[18] Hockel M, Vaupel P. Tumor hypoxia: definitions and current clinical, biologic, and molecular aspects. J Natl Cancer Inst 2001;93:266–76.

[19] Hodgkiss RJ, Jones G, Long A, et al. Flow cytometric evaluation of hypoxic cells in solid experimental tumours using fluorescence immunodetection. Br J Cancer 1991;63:119–25.

[20] Jenkins WT, Evans SM, Koch CJ. Hypoxia and necrosis in rat 9L glioma and Morris 7777 hepatoma tumors: comparative measurements using EF5 binding and Eppendorf needle electrode. Int J Radiat Oncol Biol Phys 2000;46:1005–17.

[21] Jordan BF, Baudelet C, Gallez B. Carbon-centered radicals as oxygen sensors for in vivo electron paramagnetic resonance: screening for an optimal probe among commercially available charcoals. MAGMA 1998;7:121–9.

[22] Josse O, Labar D, Georges B, Gregoire V, Marchand-Brynaert J. Synthesis of [^{18}F]-labeled EF3 [2-(2-nitroimidazol-1-yl)-N-(3,3,3-trifluoropropyl)-acetamide], a marker for PET detection of hypoxia. Bioorg Med Chem 2001;9:665–75.

[23] Kaanders JHAM, Wijffels KIEM, Marres HAM, et al. Pimonidazole binding and tumor vascularity predict for treatment outcome in head and neck cancer. Cancer Res 2002;62:7066–74.

[24] Kachur AV, Dolbier WR, Evans SM, et al. Synthesis of new hypoxia markers EF1 and [F-18]-EF. Appl Radiat Isotopes 1999;51:643–50.

[25] Kavanagh MC, Tsang V, Chow S, et al. A comparison in individual murine tumors of techniques for measuring oxygen levels. Int J Radiat Oncol Biol Phys 1999;44:1137–46.

[26] Kennedy AS, Raleigh JA, Perez GM, et al. Proliferation and hypoxia in human squamous cell carcinoma of the cervix: first report of combined immunohistochemical assays. Int J Radiat Oncol Biol Phys 1997;37:897–905.

[27] Koch CJ, Evans SM, Lord EM. Oxygen dependance of cellular uptake of EF5 [2-(2-nitro-1H-imidazol-1yl)-N-(2,2,3,3,3-pentafluoropropyl)acetamide]: analysis of drug adducts by fluorescent antibodies vs. bound radioactivity. Br J Cancer 1995;72:869–74.

[28] Koch CJ, Hahn SM, Rockwell Jr K, Covey JM, McKenna WG, Evans SM. Pharmacokinetics of EF5 [2-(2-nitro-1-H-imidazol-1-yl)-N-(2,2, 3,3,3-pentafluoropropyl) acetamide] in human patients: implications for hypoxia measurements in vivo by 2-nitroimidazoles. Cancer Chemother Pharmacol 2001;48:177–87.

[29] Laughlin KM, Evans SM, Jenkins WT, et al. Biodistribution of the nitroimidazole EF5 (2-[2-nitro-1H-imidazol-1-yl]-N-(2,2,3,3,3-pentafluoropropyl) acetamide) in mice bearing subcutaneous EMT6 tumors. J Pharmacol Exp Ther 1996;277:1049–57.

[30] Lee J, Siemann DW, Koch CJ, Lord EM. Direct relationship between radiobiological hypoxia in tumors and monoclonal antibody detection of EF5 cellular adducts. Int J Cancer 1996;67:372–8.

[31] Lord EM, Harwell L, Koch CJ. Detection of hypoxic cells by monoclonal antibody recognizing 2-nitroimidazole adducts. Cancer Res 1993;53:5271–6.

[32] Mader K, Gallez B, Swartz HM. In vivo EPR: an effective new tool for studying pathophysiology, physiology and pharmacology. Appl Radiat Isot 1996;47:1663–7.

[33] Mason RP, Antich PP, Babcock EE, Constantinescu A, Peschke P, Hahn EW. Non-invasive determination of tumor oxygen tension and local variation with growth. Int J Radiat Oncol Biol Phys 1994;29: 95–103.

[34] Maxwell PH, Dachs GU, Gleadle JM, et al. Hypoxia-inducible factor-1 modulates gene expression in solid tumors and influences both angiogenesis and tumor growth. Proc Natl Acad Sci USA 1997;94: 8104–9.

[35] Milas L, Hunter N, Mason K, Withers HR. Immunological resistance to pulmonary metastases in C3Hf/Bu mice bearing syngeneic fibrosarcoma of different sizes. Cancer Res 1974;34:61–71.

[36] Milas L, Wike J, Hunter N, Volpe J, Basic I. Macrophage content of murine sarcomas and carcinomas: association with tumor growth parameters and tumor radiocurability. Cancer Res 1987;47:1069–75.

[37] Nilges MJ, Walczak T, Swartz HM. One GHz in vivo ESR spectrometer operating with a surface probe. Phys Med 1989;2: 195–201.

[38] O'Hara JA, Lee I, Goda F, Demidenko E, Swartz HM. Effect of regrowth delay in a murine tumor of scheduling split-dose irradiation based on direct pO_2 measurements by electron paramagnetic resonance oximetry. Radiat Res 1998;150:549–56.

[39] Olive PL, Luo CM, Banath JP. Local hypoxia is produced at sites of intratumour injection. Br J Cancer 2002;86:429–35.

[40] Raleigh JA, Koch CJ. The importance of thiols in the reductive binding of 2-nitroimidazoles to macromolecules. Biochem Pharmacol 1990;40:2457–64.
[41] Raleigh JA, Dewhirst MW, Thrall DE. Measuring tumor hypoxia. Sem Radiat Oncol 1996;6:37–40.
[42] Raleigh JA, Chou SG, Arteel GE, Horsman MR. Comparisons among pimonidazole binding, oxygen electrode measurements, and radiation response in C3H mouse tumors. Radiat Res 1999;151:580–9.
[43] Rasey JS, Koh WJ, Evans ML, et al. Quantifying regional hypoxia in human tumors with positron emission tomography of [^{18}F]Fluoromisonidazole: a pretherapy study of 37 patients. Int J Radiat Oncol Biol Phys 1996;36:417–28.
[44] Rofstad EK, Halsor EF. Hypoxia-associated spontaneous pulmonary metastasis in human melanoma xenografts: involvement of microvascular hot spots induced in hypoxic foci by interleukin 8. Br J Cancer 2002;86:301–8.
[45] Stone HB, Brown JM, Phillips TL, Sutherland RM. Oxygen in human tumors: correlations between methods of measurements and response to therapy. Radiat Res 1993;136:422–34.
[46] Swartz HM, Dunn J, Grinberg O, O'Hara J, Walczak T. What does EPR oximetry with solid particles measures – and how does this relate to other measures of pO_2? Adv Exp Med Biol 1997;428:663–70.
[47] Tannock IF. The relation between cell proliferation and the vascular system in a transplanted mouse mammary tumour. Br J Cancer 1968; 22:258–73.
[48] Thomlison RH, Gray LH. The histological structure of some human lung cancers and the possible implications for radiotherapy. Br J Cancer 1955;9:539–49.
[49] Woods ML, Koch CJ, Lord EM. Detection of individual hypoxic cells in multicellular spheroids by flow cytometry using the 2-nitroimidazole, EF5, and monoclonal antibodies. Int J Radiat Oncol Biol Phys 1996;34:93–101.
[50] Young SD, Hill RP. Effects of reoxygenation on cells from hypoxic regions of solid tumors: anticancer drug sensitivity and metastatic potential. J Natl Cancer Inst 1990;82:371–80.